Atmospheric radiative transfer through global arrays of 2D clouds

J. N. S. Cole,[1] H. W. Barker,[1] W. O'Hirok,[2] E. E. Clothiaux,[3] M. F. Khairoutdinov,[4] and D. A. Randall[4]

Received 24 April 2005; revised 4 August 2005; accepted 31 August 2005; published 15 October 2005.

[1] Shortwave and longwave 2D radiative transfer calculations were performed using Monte Carlo radiative transfer models and output from a global climate model (GCM) that employed, in each of its columns, a 2D cloud system-resolving model (CSRM) with a horizontal grid-spacing Δx of 4 km. CSRM output were sampled every 9 hours for December 2000. Radiative fluxes were averaged to the GCM's grid. Monthly-mean top of atmosphere (TOA) shortwave flux differences between 2D radiative transfer and the Independent Column Approximation (ICA) are at most 5 W m^{-2} in the tropics with a zonal-average of 1.5 W m^{-2}. These differences are 2 to 10 times smaller than those stemming from the maximum-random overlap model and neglect of horizontal variability of cloud. Corresponding longwave differences are approximately 3 times smaller than their shortwave counterparts. Use of CSRM data with Δx < 4 km may roughly double the reported differences between 2D and ICA TOA SW fluxes. **Citation:** Cole, J. N. S., H. W. Barker, W. O'Hirok, E. E. Clothiaux, M. F. Khairoutdinov, and D. A. Randall (2005), Atmospheric radiative transfer through global arrays of 2D clouds, *Geophys. Res. Lett.*, *32*, L19817, doi:10.1029/2005GL023329.

1. Introduction

[2] Atmospheric scientists have long been simulating the transfer of shortwave (SW) and longwave (LW) radiation through cloudy atmospheres that exhibit variability in three spatial dimensions [*Van Blerkom*, 1971; *Welch and Wielicki*, 1984; *O'Hirok and Gautier*, 1998; *Barker et al.*, 1999]. Radiative transfer through these atmospheres represent a challenge for both inverse and forward problems. Of concern here is the forward problem faced by global climate models (GCMs) in which mean flux profiles are required for columns with cross sectional areas that typically exceed 10^4 km^2. Since both the radiative transfer process and cloud fields are unresolved over a wide range of scales in GCMs, it is often assumed that clouds are horizontally homogeneous and abide by simple rules for vertical alignment [*Barker et al.*, 2003; Q. Fu, personal communication, 2005]. Moreover, there seems little rationale, due to current computational constraints, to expect GCMs to utilize anything more sophisticated than the Independent Column Approximation (ICA) in which a 1D solution of the radiative transfer equation is applied to subcolumns that portray parametrized one-point statistical properties of unresolved clouds [*Barker et al.*, 2003]. In other words, GCMs will be neglecting 3D RT effects for the foreseeable future.

[3] In the meantime it is worthwhile to have an estimate of the magnitude of 3D radiative transfer effects that are being, and will continue to be, neglected by GCMs. But this requires a global description of cloud structure. It appears that production of a reliable, and suitable, dataset of this kind from observations made by satellite-based active-passive sensor systems (e.g., NASA's CloudSat-Calipso-AQUA triad or ESA's EarthCARE) is still several years off [*Stephens et al.*, 2002]. Currently, however, model output generated by GCMs that employ the Multi-scale Modeling Framework (MMF) for parametrization of cloud processes [*Randall et al.*, 2003] can facilitate at least a first-order estimate of the neglect of 3D radiative transfer effects by GCMs. Current configurations of MMF-GCMs employ 2D cloud system-resolving models (CSRMs) with horizontal grid-spacings of ~4 km. Therefore, radiative transfer computations are also 2D. But for diurnal-mean fluxes averaged over large horizontal areas, differences between 2D and 3D radiative transfer computations are small [*Barker*, 1996; *Cole*, 2005; *Pincus et al.*, 2005].

[4] The objective of this study is to use a month's worth of MMF-GCM output to estimate global distributions of radiative biases, at the horizontal resolution of a typical GCM cell, incurred by neglect of 2D/3D radiative transport for unresolved clouds. Radiative fluxes obtained by 2D Monte Carlo photon transport codes are compared to ICA estimates (the realistic standard for conventional GCMs) as well as estimates from two other models used by GCMs to approximate subgrid-scale cloud structure.

2. Models and Data

2.1. Cloud Data From the MMF-GCM

[5] The GCM used for this study was the National Center for Atmospheric Research (NCAR) Community Atmosphere Model (CAM - version 1.8) [*Blackmon et al.*, 2001]. For these experiments, the CAM was run at T42 horizontal resolution (~2.8° grid-spacing), with 26 layers reaching up to 3.5 hPa, and a timestep of 1 hour. The CAM's conventional 1D cloud parametrization was replaced with a 2D CSRM [*Khairoutdinov and Randall*, 2003] in each of its 8192 columns.

[6] CSRM domains have 64 columns with 4 km horizontal grid-spacing Δx, 24 vertical layers, use a timestep of 20 s, and are aligned east to west. Each CSRM was forced by large-scale tendencies updated every CAM time step, and provided horizontally averaged tendencies back to the

[1]Cloud Physics and Severe Weather Research Division, Meteorological Service of Canada, Downsview, Ontario, Canada.
[2]Institute for Computational Earth System Science (ICESS), University of California, Santa Barbara, California, USA.
[3]Department of Meteorology, Pennsylvania State University, University Park, Pennsylvania, USA.
[4]Department of Atmospheric Science, Colorado State University, Fort Collins, Colorado, USA.

0094-8276/05/2005GL023329$05.00

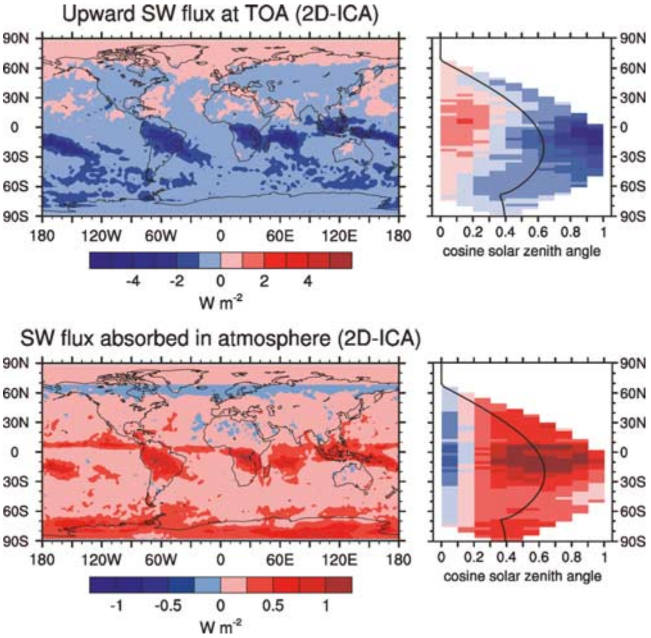

Figure 1. Maps representing differences for monthly-mean upward SW flux at TOA and SW flux absorbed by the atmosphere when radiation calculations are done with the ICA and 2D radiative transfer. Global mean values are 104.7 W m^{-2} and 73.6 W m^{-2} for upward flux at TOA and flux absorbed by the atmosphere, respectively. Plots on the right are corresponding mean values as a function of cosine of solar zenith angle μ_0 and latitude. Solid lines indicate monthly-mean μ_0.

CAM. The CSRM prognostic thermodynamic variables included liquid/ice water moist static energy, total non-precipitating water, and total precipitating water. Mixing ratios for cloud liquid, ice, rain, snow, and graupel were diagnosed as functions of temperature. All simulations started on September 1, 2000. Global arrays of CSRM data were sampled and saved every 9 model hours. Allowing the model a short spin-up period, radiation calculations were performed on model output from December 2000.

2.2. Radiative Transfer Models

[7] Four sets of radiative transfer calculations were performed for both the SW and LW. First, 3D Monte Carlo photon transport algorithms [*Cole*, 2005] were applied to the 2D CSRM fields. For the solar code, all photons were injected along the east-west plane regardless of latitude and time of day. The second set of calculations used the independent column approximation (ICA) to compute radiative heating rates for each GCM column. For the ICA, radiative fluxes and heating rates were computed for each CSRM column with the domain average computed by simply linearly averaging the column-by-column computations. Since the ICA uses CSRM fields directly, it makes no assumptions about cloud overlap and horizontal variability. For consistency, the Monte Carlo algorithms were used for both the ICA and 2D radiative transfer calculations.

[8] For the third set of calculations, cloud water contents in the CSRM fields were averaged horizontally across each layer with mean cloud water content going into each cloudy CSRM cell. The location of the cloudy cells remained the same as in the CSRM fields and therefore the vertical overlap of cloud was unchanged relative to the CSRM fields. This case will be referred to as "perfect overlap". The ICA was used to compute domain-average fluxes. The fourth set of calculations used profiles of cloud fraction and mean water contents to generate cloud fields that obey the maximum-random overlap rule using a stochastic cloud generator [*Räisänen et al.*, 2004]. Again, the clouds contained horizontally averaged cloud water contents, and domain-average fluxes were computed with the ICA. When comparing results from these last two models to ICA calculations on the original CSRM fields, all three employed the same analytic two-stream radiative transfer solver (see *Räisänen and Barker* [2004] for details). A two-stream radiative transfer solver was used in conjunction with the stochastic cloud generator to keep the computation time reasonable. To reduce stochastic noise in radiative heating rates and fluxes, mean values were computed based on 10-member ensembles of the cloud fields. Therefore, when two sets of radiative transfer calculations are compared, both sets derive from a common radiative transfer solver; either a Monte Carlo algorithm or an analytic two-stream.

[9] All radiative transfer models employed here used the same parametrizations for gaseous transmittances and cloud optical properties. The correlated *k*-distribution method was used to parametrize gaseous transmittances while liquid and ice cloud optical properties were based on polynomial fits to Mie calculations [*Cole*, 2005].

3. Results

[10] The upper portion of Figure 1 shows monthly-mean maps of differences between 2D radiative transfer and the ICA for upwelling SW at the top of atmosphere (TOA). As expected, the largest impacts on albedo are associated with tropical deep convective clouds. Secondary maxima occur across the southern ocean storm belt partly because of excessive cloudiness and large solar inputs. The accompanying plot shows the distribution of flux differences as a function of latitude and cosine of solar zenith angle μ_0. Suppression of photon leakage out the sides of convective clouds in the ITCZ at large μ_0 is responsible for large enhancements of albedo when 2D radiative transfer is neglected. Conversely, the ICA does not account for side illumination of these clouds, so at small μ_0 it under estimates albedo significantly [cf. *Welch and Wielicki*, 1984; *O'Hirok and Gautier*, 1998].

[11] The map in the lower portion of Figure 1 shows SW atmospheric absorption differences which are much smaller than differences at the TOA. They are, however, strongly biased towards 2D effects increasing absorption and being more confined to convective clouds in the ITCZ and vertically extensive, mesoscale-sized ice clouds over Antarctica. The corresponding latitude-μ_0 distribution indicates that the largest increases occur for intermediate values of μ_0 due to the effects of cloud-side illumination (note that for December, μ_0 are always intermediate over Antarctica). Vertical cross sections of monthly mean SW heating rate differences between 2D and ICA are shown in Figure 2.

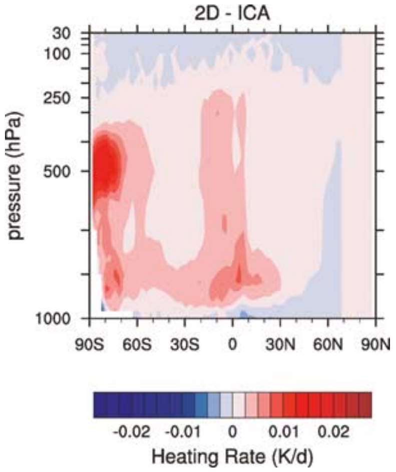

Figure 2. Monthly-mean cross section of differences in SW heating rate between 2D radiative transfer and the ICA as a function of latitude and altitude.

These show clearly the impact of cloud side illumination at cloud-bearing altitudes.

[12] Figure 3 puts into context differences between 2D and ICA cloud radiative effects (CRE) at TOA for SW and LW radiation. Note that the effect of 2D radiative transfer in the LW is very small. In addition to 2D and ICA differences, Figure 3 shows differences between ICA calculations using the cloud fields directly from the CSRM and clouds in perfect overlap configuration. Perfect overlap means that clouds from the CSRM are homogenized horizontally using layer mean cloud water contents but cloud positions are unchanged relative to the CSRM fields. These differences illustrate the impact of neglecting horizontal variations, which for the SW is roughly 5 times larger than the corresponding impact going from 2D to ICA. Also shown are differences between ICA and homogeneous clouds that obey the maximum-random overlap rule (which is popular with GCM groups). Note how effectively the maximum-random overlap assumption counters homogenization, especially in the tropics. Still, however, the impact of the maximum-random overlap in the SW is 2 to 3 times larger than the 2D effect; in the LW it towers over the meager 2D effect.

[13] At this stage, a crucial question is: since all ICA and 2D radiative transfer fluxes have been computed using Δx = 4 km, how should these differences be scaled to represent differences at smaller Δx? There are two ways to go about investigating this: by assessing either $\alpha_{2D}(\Delta x) - \alpha_{ICA}(\Delta x)$ or $\alpha_{2D}(\Delta x) - \alpha_{ICA}$ (5 km) km, where α denotes broadband, domain-average TOA albedo. The former illustrates direct differences between 2D and ICA as a function of Δx. The latter addresses the more immediate question of differences between ICA applied at current (semi-operational) MMF grid-spacings and 2D at much higher resolution.

[14] To get an estimate of how results presented thus far might scale as a function of Δx, six cloud fields were considered whose properties were inferred from passive/active radiometric measurements made at various Atmospheric Radiation Measurement sites [*O'Hirok and Gautier*, 2005]. Owing to their relative magnitude, results are shown only for SW fluxes. Figure 4a shows $\alpha_{2D}(\Delta x) - \alpha_{ICA}(\Delta x)$ as a function of Δx. The underlying message here is that albedo differences are almost eliminated entirely at Δx = 20 km, but at Δx = 4 km they are very close to those at 0.2 km, with the exception of towering cumulonimbus. It is unlikely that the situations change much for smaller values of Δx where $\partial F_{2D}/\partial\Delta x \approx \partial F_{ICA}/\partial\Delta x \approx 0$. Moreover, differences for $\Delta x \leq 5$ km indicate, once again, that use of the ICA to obtain domain averages should suffice for most Δx.

[15] Figure 4b shows $\alpha_{2D}(\Delta x) - \alpha_{ICA}$(5 km). It can be seen that differences at Δx = 0.2 km can be several times larger than at 4 km for cumuliform clouds, and about double for the others. Thus, once all-sky conditions (including cloudless skies) are factored in (i.e., to produce zonal averages), the magnitude of the bias due to neglect of 2D radiative transfer relative to ICA at 4 km may be magnified approximately by a factor of 2. This is similar for surface absorptance. Corresponding results for total atmospheric absorptance (not shown) show much weaker dependencies on Δx and so values presented thus far are likely to be very close to the ultimate 2D effect.

[16] The shaded line in Figure 3 indicates a scaling of the 2D - ICA curve by a factor of 2. This approximates the likely upper limit of the impact of neglecting full 2D radiative transfer effects relative to ICA performed at Δx = 4 km. The implication is that neglect of 2D radiative transfer

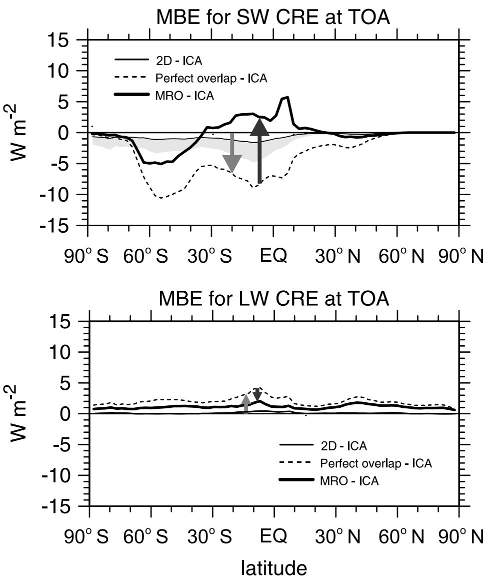

Figure 3. Zonal-average, monthly-mean differences in SW (top) and LW (bottom) cloud radiative effect (CRE) between the full ICA and three other models. Grey arrow indicates the impact of neglecting horizontal variations in cloud water while maintaining the overlap from the CSRMs (Perfect overlap). Black arrow represents the impact of forcing homogeneous clouds to follow the maximum-random overlap (MRO) rule. If on the SW plot the thin solid line's values (2D - ICA) are scaled by values between one and two, the result is the grey region which represents the estimated difference between performing ICA calculations with 4 km data verses 2D radiative transfer using data resolved down to at least 200 m.

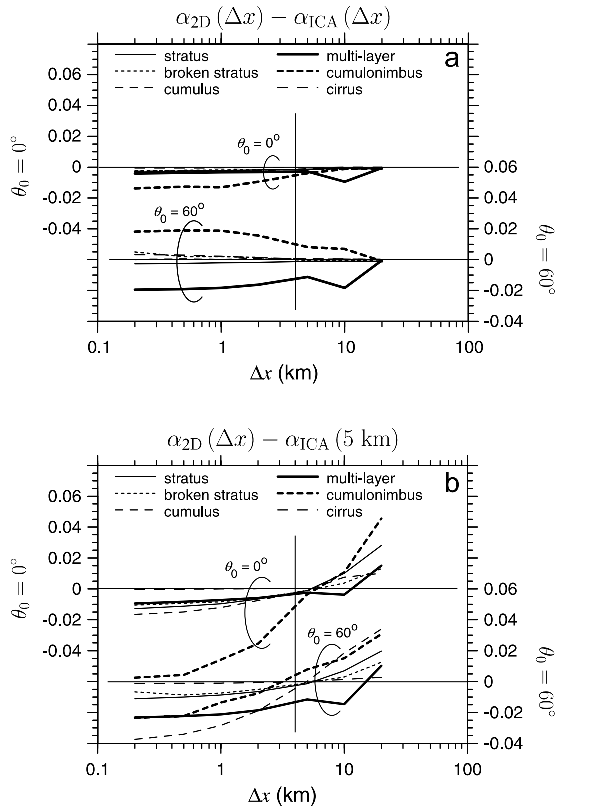

Figure 4. (a) Broadband, TOA albedo α differences predicted by a 2D transfer algorithm and the ICA as a function of horizontal grid-spacings Δx. (b) Similar to (a) except this shows differences between 2D transfer at various Δx and the ICA at $\Delta x = 5$ km. Results are shown for two solar zenith angle θ_0 and six distinct cloud fields.

effects at 4 km resolution is beginning to rival the impact of the maximum-random overlap method. The essential difference is that, on average, neglect of 2D effects result in one-sided biases whereas the bias errors due to the maximum-random overlap rule reverse sign as a function of latitude.

4. Conclusions

[17] The intention here was to estimate the radiative impact, on a global scale, of neglecting 2D radiative transfer and cloud structure at the grid-spacing commonly used in global climate models. Due to computational limitations, only diagnostic radiative transfer calculations were performed. Assessing the impact on simulated climate is impractical at present, and may be so for some time. Moreover, model output generated by a global array of 2D CSRMs had to be used as suitable observational data do not exist, and may not for some time.

[18] As expected, neglect of 2D radiative transfer and cloud structure is greatest in the SW with maximal impacts occurring in the ITCZ, where towering convective clouds are common, and for intermediate to small solar zenith angles, where cloud side illumination can be significant. Using cloud data resolved at 4 km horizontal resolution, the radiative impact of neglecting 2D radiative transfer is about 2 to 3 times smaller than that associated with making the popular maximum-random overlap assumption. If, however, one considers cloud fields with grid-spacings smaller than 4 km, the bias resulting from neglect of 2D radiative transfer relative to the ICA begins to rival that of the maximum-random overlap approximation.

[19] Solutions to this problem depend in part on the application. For MMF-GCMs, one could apply 2D radiative transfer solvers to the highly resolved CSRM cloud fields produced within. If the CSRMs in these GCMs continue to be resolved at scales near 4 km, a statistical allowance seems warranted to account for fluctuations that are still unresolved. This allowance could include a scaling of optical properties thereby accounting for unresolved fluctuations [e.g., *Rossow et al.*, 2002]. As for conventional GCMs, a Monte Carlo ICA approach in conjunction with a 1-point stochastic cloud generator will take one only as far as the full ICA [*Barker et al.*, 2003; *Räisänen and Barker*, 2004]. The next step would be application of 2D photon transport solvers to stochastically-generated unresolved 2D subgrid-scale clouds [e.g., *Venema et al.*, 2004].

[20] **Acknowledgments.** This study was supported by a grant from the US Department of Energy (Atmospheric Radiation Measurement (ARM) grant DE-FG02-05ER63955), and the Modelling of Clouds and Climate Proposal funded through the Canadian Foundation for Climate and Atmospheric Sciences, the Meteorological Service of Canada, and the Natural Sciences and Engineering Research Council.

References

Barker, H. W. (1996), A parameterization for computing grid-averaged solar fluxes for inhomogeneous marine boundary layer clouds. part I: Methodology and homogeneous biases, *J. Atmos. Sci.*, *53*, 2289–2303.

Barker, H. W., G. L. Stephens, and Q. Fu (1999), The sensitivity of domain-averaged solar fluxes to assumptions about cloud geometry, *Q. J. R. Meteorol. Soc.*, *125*, 2127–2152.

Barker, H. W., et al. (2003), Assessing 1D atmospheric solar radiative transfer models: Interpretation and handling of unresolved clouds, *J. Clim.*, *16*, 2676–2699.

Blackmon, M., et al. (2001), The Community Climate System Model, *Bull. Am. Meteorol. Soc.*, *82*, 2357–2376.

Cole, J. N. S. (2005), Assessing the importance of unresolved cloud-radiation interactions in atmospheric global climate models using the multi-scale modelling framework, Ph.D. thesis, Pa. State Univ., University Park.

Khairoutdinov, M. F., and D. A. Randall (2003), Cloud resolving modeling of the ARM summer 1997 IOP: Model formualation, results, uncertainties, and sensitivities, *J. Atmos. Sci.*, *60*, 607–625.

O'Hirok, W., and C. Gautier (1998), A three-dimensional radiative transfer model to investigate the solar radiation within a cloudy atmosphere. part I: Spatial effects, *J. Atmos. Sci.*, *55*, 2162–2179.

O'Hirok, W., and C. Gautier (2005), The impact of model resolution on differences between independent column approximation and Monte Carlo estimates of shortwave surface irradiance and atmospheric heating rate, *J. Atmos. Sci.*, *62*, 2939–2951.

Pincus, R., C. Hannay, and K. F. Evans (2005), The accuracy of determining three-dimensional radiative transfer effects in cumulus cloud using ground-based profiling instruments, *J. Atmos. Sci.*, *62*, 2284–2293.

Räisänen, P., and H. W. Barker (2004), Evaluation and optimization of sampling errors for the Monte Carlo Independent Column Approximation, *Q. J. R. Meteorol. Soc.*, *130*, 2069–2085.

Räisänen, P., H. W. Barker, M. F. Khairoutdinov, J. Li, and D. A. Randall (2004), Stochastic generation of subgrid-scale cloudy columns for large-scale models, *Q. J. R. Meteorol. Soc.*, *130*, 2047–2068.

Randall, D. A., M. F. Khairoutdinov, A. Arakawa, and W. W. Grabowski (2003), Breaking the cloud-parameterization deadlock, *Bull. Am. Meteorol. Soc.*, *84*, 1547–1564.

Rossow, W. B., C. Delo, and B. Cairns (2002), Implications of the observed mesoscale variations of clouds for the Earth's radiation budget, *J. Clim.*, *15*(65), 557–585.

Stephens, G. L., et al. (2002), The CloudSat mission and the A-train: A new dimension of space-based observations of clouds and precipitation, *Bull. Am. Meteorol. Soc.*, *83*, 1771–1790.

Van Blerkom, D. J. (1971), Diffuse reflection from clouds with horizontal inhomogeneities, *Astrophys. J.*, *166*, 235–242.

Venema, V., S. Meyer, S. G. García, A. Kniffka, C. Simmer, S. Crewell, U. Löhnert, T. Trautmann, and A. Macke (2004), Iterative amplitude adapted Fourier transform surrogate cloud fields, paper presented at 14th International Conference on Clouds and Precipitation, World Meteorol. Organ., Bologna, Italy, 18–23 July.

Welch, R. M., and B. A. Wielicki (1984), Stratocumulus cloud field reflected fluxes: The effect of cloud shape, *J. Atmos. Sci.*, *41*, 3085–3103.

H. W. Barker and J. N. S. Cole, Cloud Physics and Severe Weather Research Division, Meteorological Service of Canada, 4905 Dufferin St., Downsview, ON, Canada M3H 5T4. (jason.cole@ec.gc.ca)

E. E. Clothiaux, Department of Meteorology, Pennsylvania State University, University Park, PA 16802, USA.

M. F. Khairoutdinov and D. A. Randall, Department of Atmospheric Science, Colorado State University, Fort Collins, CO 80523, USA.

W. O'Hirok, Institute for Computational Earth System Science (ICESS), University of California, Santa Barbara, CA 93106, USA.